

## A Multilevel Inverter Based on SVPWM Technique for Photovoltaic Application

**Shantanu Chatterjee**

School of Electrical Engineering, VIT University, Vellore, India  
e-mail:instru59engg@gmail.com

---

### Article Info

#### Article history:

Received Apr 29, 2012

Revised Jan 7, 2013

Accepted Jan 24, 2013

---

#### Keyword:

Labview

NPC

PV cell

SVPWM

Two-level three phase inverter

---

### ABSTRACT

Multilevel inverters can reach the increasing demand for power quality and power ratings along with lower harmonic distortion and lesser electromagnetic interference (EMI). As the number of levels increases, it is important to control more switches in parallel with their concurrent processing capability. In this paper space vector pulse width modulation (SVPWM) Technique is proposed for the two-level and three-level neutral point clamped (NPC) inverter. Due to the geometrical symmetry of six sectors, there will be close relationship between on-time arrangements and on-time calculations for switches respectively. The two and three level inverter is simulated using MATLAB/Simulink and also the experimental results are presented for verifying the effectiveness of the system. The use of Photovoltaic Cell as source for the NPC Inverter is proposed here in this paper.

*Copyright © 2013 Institute of Advanced Engineering and Science.  
All rights reserved.*

---

### Corresponding Author:

**Shantanu Chatterjee**

School of Electrical Engineering, VIT University, Vellore, India  
e-mail:instru59engg@gmail.com

---

## 1. INTRODUCTION

The ever growing demand for Renewable Energy resources is gaining importance day by day. Wind, Solar, Nuclear, Hydral etc are some examples of such renewable energies. It is expected that by 2050, 60% of our energy requirement will be supplied by these Renewable energy resources. Out of these PV Energy has been used in most number of cases as it is distributed over the whole area of the earth and it is available in sufficient amount.

Due to this reason now our focus is on inventing new tropologies of improved inverters. Among these tropologies multilevel inverter with PWM control is gaining more importance. They have many additional advantages over the other tropologies and are more efficient.

The Pulse Width Modulation Technique is also called as "Vector Modulation", which is based on space vector theory, became the most important development in the recent years. Even though, many no of pulse width modulation (PWM) methods are created before, the vector modulation technique seems to be the best alternative method for a three phase switching inverter, current control applied to converters, loop testing in real-time hardware for control design, in controller implementation, in recovering and separating independent source signals, and in neural computation. As the conceptual method of multilevel PWM converter was introduced, several modulation techniques have been studied and developed in detail, such as multilevel SPWM, SVPWM and multilevel selective harmonic elimination. In these methods, the space vector PWM comes out because it gives significant flexibility in optimizing the switching waveforms and suitable for digital implementation.

## 2. NPC INVERTER

Block diagram of the multilevel inverter based on SVPWM technique is shown in the fig.1 Type of multilevel inverter used in this paper is NPC three-level inverter. DC voltage source supplies input voltage to the multilevel inverter and it is controlled by the series of pulses based on ON and OFF times of the corresponding. Switches in the respective legs of the NPC inverter these switching pulses of switches are given by the SVPWM algorithm. The output voltage from the multilevel inverter is given to load

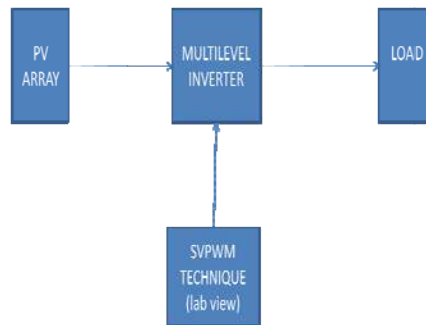


Figure 1. Block Diagram

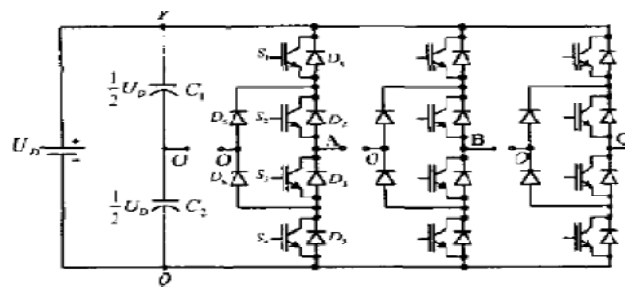


Figure 2. Schematic of the Neutral-Point-Clamped three-level Inverter

Among the multilevel inverters which has gained much attention and frequently used is the Neutral-Point- Clamped (NPC) multilevel inverter or also called as Diode-Clamped multilevel inverter. This inverter was first proposed by Nabae ET. Fig.2 shows the three-level NPC inverter.

Normally, NPC multilevel inverter gives the small step of staircase output voltage from many levels of DC capacitor voltages. An n-level NPC inverter comprises of (n-1) capacitors on the DC bus,  $2(n-2)$  clamping diodes per phase and  $2(n-1)$  switches per phase. Fig.2 shows the structure of 3-level NPC inverter. The DC bus voltage is divided into three voltage levels with help of two DC capacitors,  $C_{a1}$  and  $C_{a2}$ . Each capacitor is having  $V_{dc}/2$  volts and each voltage stress will be limited to one capacitor level with help of clamping diodes. The output voltage,  $V_{an}$  is having 3 states as given in [2].

The no of levels can be increased to a high level by adding switches and with this, the inverter will be getting high AC voltage, producing several no of voltage steps that will be reaching sinusoidal with lower harmonic distortion. In the time of inverter operation, the switching devices near the center tap point are switched ON for a longer duration compared to the switching devices further away from the center tap point as shown in the switching states. As the switching device is further away from the center tap point the switching time is for shorter duration. Other difference among the normal conventional two-level inverter and multilevel NPC inverter is the clamping diode (D) in the phase. In case of three-level NPC inverter, clamping diode in the phase A,  $D_{a1}$  and  $D_{a4}$  clamped the DC bus voltage in phase A into 3 voltage levels which are  $+V_{dc}/2$ , 0 and  $-V_{dc}/2$ . Diode,  $D_{a4}$  in phase A balancing the sharing of voltage between  $S_{a4in}$  and  $S_{a4out}$ ; with  $S_{a4in}$  stopping the voltage across  $C_{a1}$  and  $S_{a4out}$  stops the voltage across  $C_{a2}$  in the phase A. The process repeats for the remaining two phase B and C.

**3. Space vector PWM Modulation**

As from the Table. 1, there are 27 switching States in NPC three-level inverter. Which corresponds to 19 voltage vectors (Vo to Vie) Positions which are fixed. These space voltage vectors are divided into four groups, which are: large space voltage vector (VI, VI, etc.), medium space voltage vector, small space voltage vector, and zero space voltage vector (Vo). The plane is divided into six major sectors ('a' to 'f') with help of large space voltage vectors and zero space voltage vectors. Each major sector denotes 60° of the fundamental cycle [4]. Within every major sector, it contains four minor regions. Totally there are 24 minor regions in the plane. And the vertex point of these regions denotes the voltage vectors. Observe the Table, each small space voltage vectors and zero space voltage vectors have 2 and 3 redundant switching states, respectively. In 3-phase 3-level inverter, when the rotating space voltage vectors falls into one particular sector, adjacent voltage vectors are selected to make the desired rotating space voltage vector based on the vector synthesis principle, as result it gives 3-phase PWM waveforms. By the observing the phase angle and the magnitude of a rotating reference voltage vector? The sector in which v\* lies can be easily find out. [5]

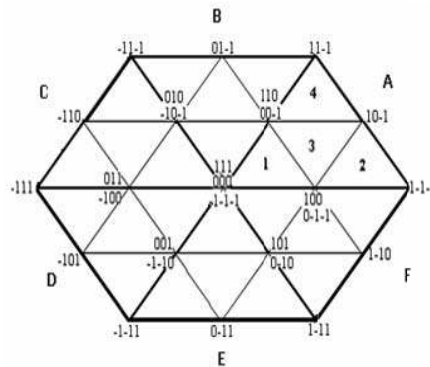


Figure 3. Space vector diagram of three-level inverter

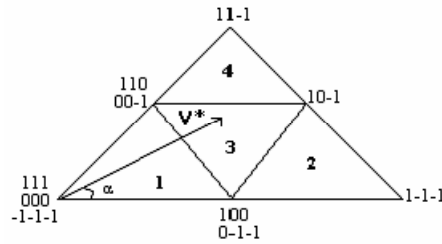
Based on the principle of SVPWM technique that the command voltage vector V\* is nearly calculated by using three adjacent vectors. The duration period of each and every voltage vectors are obtained by following vector calculations;  
 $T1V1 + T2V2 + T3V3 = TsV$   
 $T1+T2+T3=Ts$

Table 1. Switching States.

| switching states | Sa | Sb | Sc | Corresponding voltage vectors |
|------------------|----|----|----|-------------------------------|
| S1               | 0  | 0  | 0  | V0                            |
| S2               | 1  | 1  | 1  | V0                            |
| S3               | 2  | 2  | 2  | V0                            |
| S4               | 1  | 0  | 0  | V1                            |
| S5               | 1  | 1  | 0  | V2                            |
| S6               | 0  | 1  | 0  | V3                            |
| S7               | 0  | 1  | 1  | V4                            |
| S8               | 0  | 0  | 1  | V5                            |
| S9               | 1  | 0  | 1  | V6                            |
| S10              | 2  | 1  | 1  | V1                            |
| S11              | 2  | 2  | 1  | V2                            |
| S12              | 1  | 2  | 1  | V3                            |
| S13              | 1  | 2  | 2  | V4                            |
| S14              | 1  | 1  | 2  | V5                            |
| S15              | 2  | 1  | 2  | V6                            |
| S16              | 2  | 1  | 0  | V7                            |
| S17              | 1  | 2  | 0  | V8                            |
| S18              | 0  | 2  | 1  | V9                            |
| S19              | 0  | 1  | 2  | V10                           |
| S20              | 1  | 0  | 2  | V11                           |
| S21              | 2  | 0  | 1  | V12                           |
| S22              | 2  | 0  | 0  | V13                           |
| S23              | 2  | 2  | 1  | V14                           |
| S24              | 0  | 2  | 0  | V15                           |
| S25              | 0  | 2  | 2  | V16                           |
| S26              | 0  | 0  | 2  | V17                           |
| S27              | 2  | 0  | 2  | V18                           |

The vectors that define the triangle region in which V\* is located are V1, V2 and V3. T1, T2 and T3 are the vector durations respectively and Ts is the sampling time.[6]  
 The three-level inverter similar to a two-level inverter in such way that, each space vector diagram is divided into 6 sectors. For simple understanding the switching patterns for Sector 'a' is defined and calculation technique is same for the other sectors. Sector 'a' is divided into four regions. Space vector pulse width modulation for three-level inverters can be implemented by the following steps ;  
 a. Find the sector in the hexagon,  
 b. Find the respective region in the sector ,  
 c. Calculate the respective switching times for ta, tb, tc ,

d. Find the switching states based on the above step,



a. Finding the sector in the hexagon:

Alfa ( $\alpha$ ) is calculated and then the sector, in which the ref vector  $V^*$  is located, is determined as;

- If  $\alpha$  is in the range of  $0^\circ \leq \alpha < 60^\circ$ , then vector  $V^*$  lies in Sector a,
- If  $\alpha$  is in the range of  $60^\circ \leq \alpha < 120^\circ$ , then vector  $V^*$  lies in Sector b,
- If  $\alpha$  is in the range of  $120^\circ \leq \alpha < 180^\circ$ , then vector  $V^*$  lies in Sector c,
- If  $\alpha$  is in the range of  $180^\circ \leq \alpha < 240^\circ$ , then vector  $V^*$  lies in Sector d,
- If  $\alpha$  is in the range of  $240^\circ \leq \alpha < 300^\circ$ , then vector  $V^*$  lies in Sector e,
- If  $\alpha$  is in the range of  $300^\circ \leq \alpha < 360^\circ$ , then vector  $V^*$  lies in Sector f.

b. Finding the respective region in the sector:

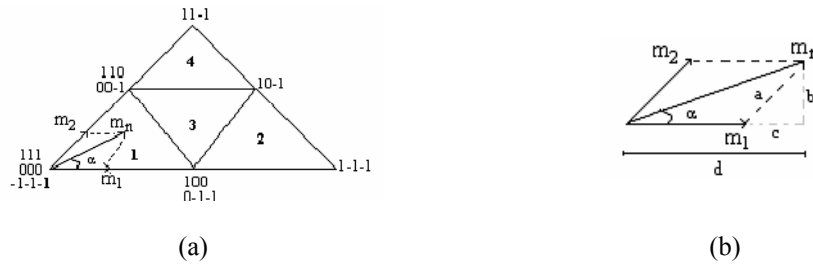


Figure 4. Space vector diagram for  $m_1$  and  $m_2$  in Sector 'a'.

From Figure 4 (b)  $m_1$  and  $m_2$  in sector 'a' can be calculated as

$$a = m_2 = \frac{b}{\sin(\pi/3)} = \frac{2}{\sqrt{3}} b = \frac{2}{\sqrt{3}} m_n \cdot \sin\alpha$$

$$m_1 = m_n \cdot \cos\alpha - \left( \frac{2}{\sqrt{3}} m_n \cdot \sin\alpha \right) \cos(\pi/3)$$

$$m_1 = m_n \left( \cos\alpha - \frac{\sin\alpha}{\sqrt{3}} \right)$$

And by,

- If the value of  $m_1, m_2$  and  $(m_1+m_2) < 0.5$ , then  $V^*$  lies in Reg 1,
- If the value of  $m_1 > 0.5$ , then  $V^*$  lies in Reg 2,
- If the value of  $m_2 > 0.5$ , then  $V^*$  lies in Reg 3,
- If the value of  $m_1$  and  $m_2 < 0.5$  and  $(m_1+m_2) > 0.5$ , then  $V^*$  lies in Reg 4.

c. Calculating the respective switching times for  $t_a, t_b, t_c$ :

$t_a, t_b, t_c$  switching times of Sector 'a' is given in

Table 2. Switching times for Sector A

|       | Region I                                | Region II                               |
|-------|---|---|
| $T_a$ | $1.1^*m^*T_s^*\sin((\pi/3)-\alpha)$     | $T_s(1-1.1^*m^*\sin(\alpha+\pi/3))$     |
| $T_b$ | $T_s/2(1-(2^*1.1^*\sin(\alpha+\pi/3)))$ | $1.1^*T_s^*m^*\sin\alpha$               |
| $T_c$ | $1.1^*T_s^*\sin\alpha$                  | $T_s/2((2^*1.1^*\sin(\pi/3-\alpha))-1)$ |
|       | Region III                              | Region IV                               |
| $T_a$ | $T_s/2(1-2^*1.1^*m^*\sin\alpha)$        | $T_s/2(2^*1.1^*m^*\sin(\alpha)-1)$      |
| $T_b$ | $T_s/2(2^*1.1^*\sin(\pi/3+\alpha)-1)$   | $1.1^*m^*T_s^*\sin((\pi/3)-\alpha)$     |
| $T_c$ | $T_s/2(1+2^*1.1^*\sin(\alpha-\pi/3))$   | $T_s(1-(1.1^*m^*\sin(\alpha+\pi/3)))$   |

d. Finding the switching states based on above step:

At any time by taking the switching transition of only one switch ; the switching transition orders are shown below and they are obtained for every region in Sector ‘a’ if all switching transition states in every region are used. Therefore, switching states for Sector ‘a’ given below

Reg 1:-1-1-1, 0-1-1, 00-1, 000, 100, 110, 111

Reg 2: 0-1-1, 1-1-1, 10-1, 100

Reg 3: 0-1-1, 11-1, 10-1, 100, 110

Reg 4: 00-1, 10-1, 11-1, 110

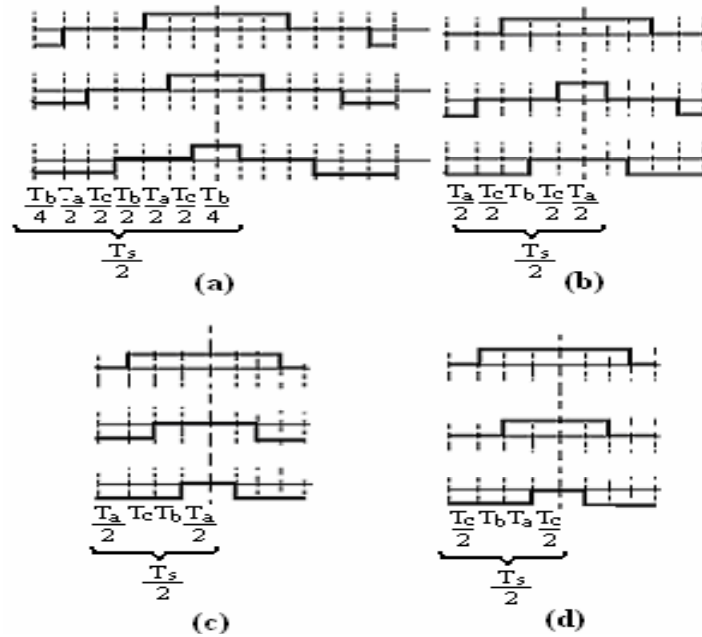


Figure 5. Switching States of Sector ‘a’: (a) Reg.1, (b) Reg 2, (c) Reg 3, (d) Reg 4.

**4. Photovoltaic Arrays**

The Photovoltaic Cells converts the solar energy of the sun to electrical energy i.e. electricity. The basic unit of a PV array is a PV cell. The PV cells grouped together to form a PV panels and these PV panels can be further grouped together to form a PV array. The PV cells [11] can be either circular or rectangular in shape. Each PV cells can be considered as a simple p-n junction diodes and the surface of these diodes are exposed directly to the sunlight and in turn the charge carriers are generated which produces electricity.

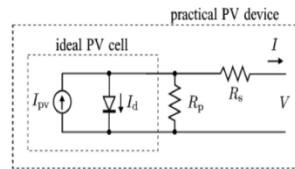


Figure 6. Basic Circuit diagram of a PV cell using one diode

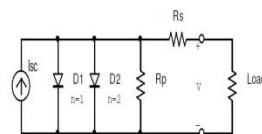


Figure 7. PV cell using two diode models.

The basic diagram of a PV cell is shown in fig.4 and to compensate the error the two diode model is also given in fig.4. In this fig the PV cell is represented by a current source and the  $R_p$  and  $R_s$  is the parallel and series resistance respectively.  $V$  and  $I$  are the output voltage and output current respectively. From the fig it is evident that the net current  $I$  is the summation of  $I_{pv}$  and  $I_d$  so

$$I = I_{pv} - I_d \tag{4}$$

Where

$$I_d = I_0 \exp(qV/akT)$$

$I_0$  = Leakage current of the diode.

$q$  = Electronic charge

$k$  = Boltzmann Constant

$T$  = Temperature of the pn junction

$a$  = Diode ideality constant

The equation (4) is the ideal equation which is a bit different from the practical one. Actually the practical PV array is composed of more than one PV cells and so the basic equation requires some additional terms. The actual eq is given below

$$I = I_{pv} - [\exp \{V + (R_s I / V_t) a\} - 1] - (V + R_s I / R_p) \tag{5}$$

Where

$$V_t = N_s kT / q$$

This is the thermal voltage of the cell with  $N_s$  no of cells connected in series. The cells connected in parallel increases the current and cells connected in series increases the voltage. The I-V characteristic [13]-[14] is shown in figure 6 below. From this figure we can easily find that the voltage and current is maximum at some point let it be called as MPP. Here as the voltage and current is maximum we can get the maximum power at this point. The voltage and current corresponding to this point is  $V_{mp}$  and  $I_{mp}$  respectively.

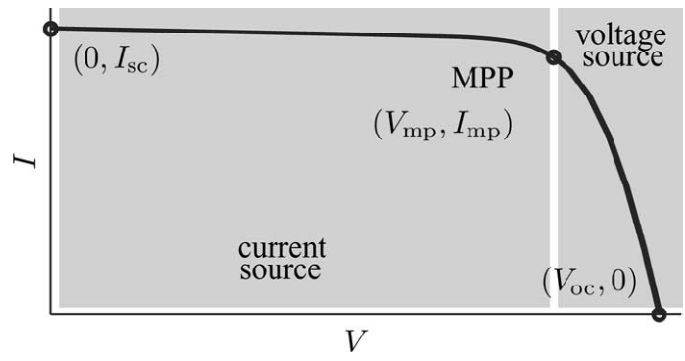


Figure 8. V-I characteristics of an PV cell

Table 3. Parameters for PV cell waree ws 100

| Parameters                           | Values                 |
|--------------------------------------|------------------------|
| Maximum Power (Pmax)                 | 10 W                   |
| Voltage at maximum Power (Vmp)       | 17 V                   |
| Current at max Power (Imp)           | 0.59 A                 |
| Open Circuit Voltage                 | 21 V                   |
| Short Circuit Current                | 0.62 A                 |
| Tolerance                            | 5%                     |
| Power Measured at Standard Test Load | 1000W/m2 ,25 c ,AM 1.5 |
| Temperature Co-efficient of Power    | -0.47 %/K              |
| Temperature Co-efficient of Voltage  | -0.123 V/K             |
| Operation Temperature                | -40 C to 85 C          |
| Nominal operating Cell temp          | 48 °C                  |
| Maximum System Voltage               | 1000VDC                |

Here in this diagram  $I_{sc}$  is known as the short circuit current i.e. the current is maximum when the output terminal is short circuited and  $V_{oc}$  is known as the open circuited voltage i.e. the voltage is maximum when the output terminal is open. Actually the output of the solar cell is not constant as the irradiance and temperature changes throughout the day and so it becomes very important for us to track this MPP i.e. maximum power point to get a very efficient and robust system. The parameter of the PV cell being used here is given in Table 3.

## 5. Matlab /Simulink model

### 5.1 Simulation of Multilevel Inverter.

The simulation diagram for Two level and three level is shown in fig. 9 and fig. 10.

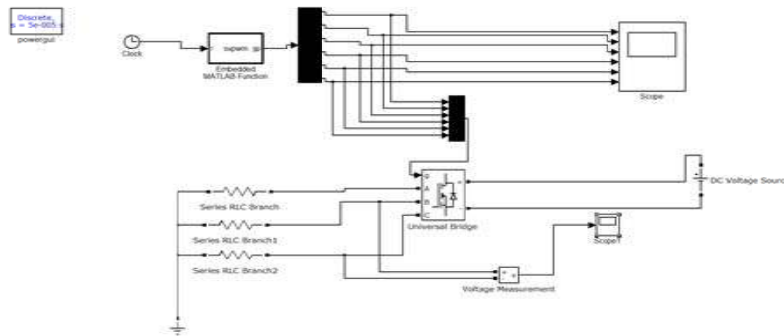


Figure 9. Two-level SVPWM inverter

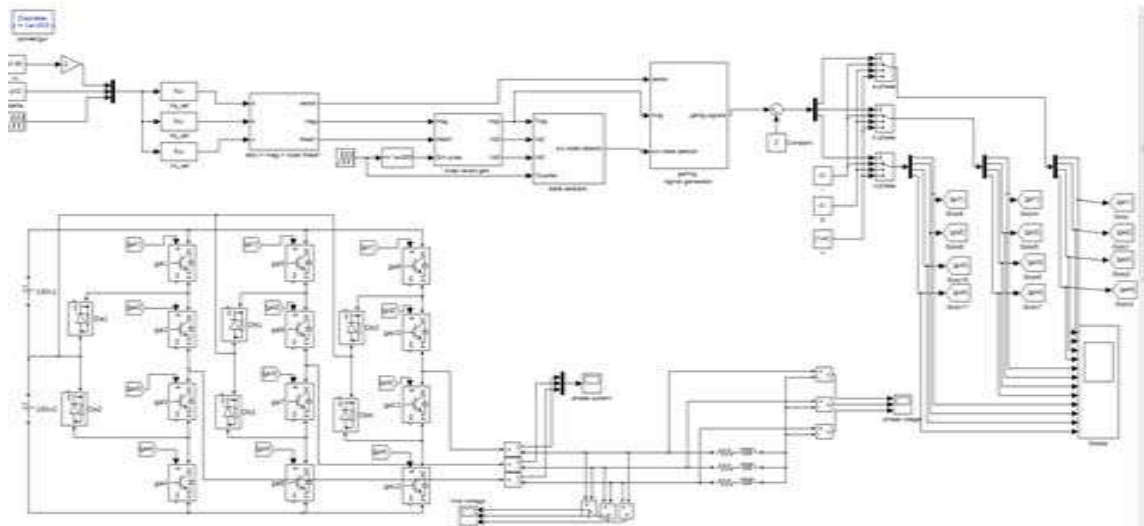


Figure 10. Three-level SVPWM inverter

### 5.2. Simulation of PV Module

In this analysis the resistance  $R_p$  is eliminated. The output voltage  $V$  can be obtained by simplifying the equation (2) which gives:-

$$V = (akT/e) \ln \left\{ \frac{I_{ph} + I_d - I}{I_d} \right\} - (R_s I) \quad (6)$$

Where

$k$  = Boltzmann Constant ( $1.38 \times 10^{-23} \text{ J/K}$ )

$e$ =electronic Charge ( $1.602 \cdot 10^{-19}C$ )

$T$ =Reference operating temperature (20 C)

$R_s$ =Series resistance (0.001 ohm)

$I_d$ =Reverse saturation current of the diode (0.0002 A)

The ambient temperature  $T_a$  affects the output voltage and photocurrent of the cell and this can be represented by two temperature coefficient  $C_{TV}$  and  $C_{TI}$  and can be represented by

$$C_{TV} = 1 + \beta_T(T_a - T_x) \tag{7}$$

$$C_{TI} = 1 + \gamma_T/S_c(T_a - T_x) \tag{8}$$

Where  $\beta_T = 0.004$  and  $\gamma_T = 0.06$  and another cell ambient temperature is  $T_x$ . Based on this two equation the Simulation is carried out.

The temperature change  $\Delta T_c$  occurs due to the change in solar irradiation level and can be given by:-

$$\Delta T_c = \alpha_c(S_x - S_c) \tag{9}$$

Where the constant  $\alpha_c$  represents the change in slope of the cell operating temperature due to change in solar irradiation level.

The new value of cell voltage  $V_{cx}$  and photocurrent  $I_{phx}$  can be obtained for new value of temperature  $T_x$  and solar irradiation  $S_x$  by the given equation:-

$$V_{cx} = C_{SV} C_{TV} V_c \tag{10}$$

$$I_{phx} = C_{SI} C_{TI} I_{ph} \tag{11}$$

Where  $C_{SV}, C_{TV}, C_{SI}, C_{TI}$  are the correlation coefficients.

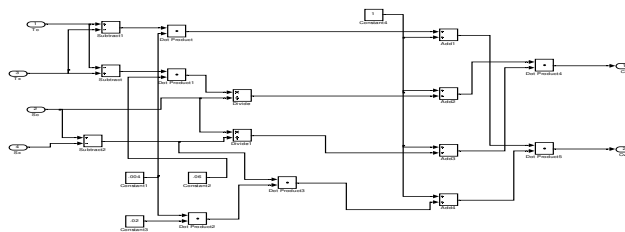


Figure 11. PV Sub-module for correction factor for current.

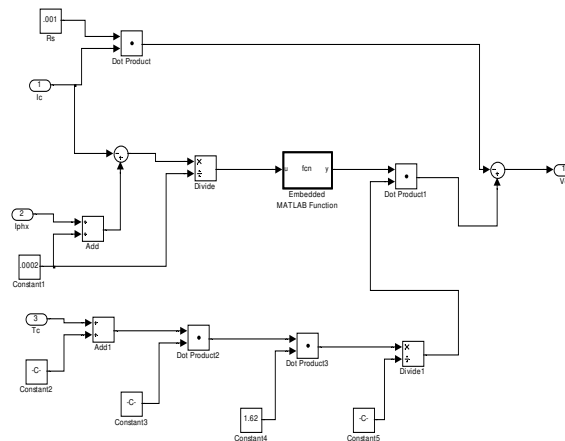


Figure 12. PV Sub module for determining the PV cell output voltage



### 1.3 Simulation of Multilevel Inverter Integrated with PV Cell by MPPT Algorithm.

In this algorithm a slight perturbation is introduced into the system. This perturbation causes the power of the solar module to change. If the power increases due to the perturbation then the perturbation is continued in that direction. After the peak power is reached the power at the next instant decreases and hence after that the perturbation reverses. When the steady state is reached the algorithm oscillates around the peak point. In order to keep the power variation small the perturbation size is kept very small. The algorithm is developed in such a manner that it sets a reference voltage of the module corresponding to the peak voltage of the module. A PI controller then acts moving the operating point of the module to that particular voltage level. It is observed that there is some power loss due to this perturbation also it fails to track the power under fast varying atmospheric conditions. But still this algorithm is very popular and simple. The PV module is connected to the inverter by a boost converter which is used to increase the DC voltage level.

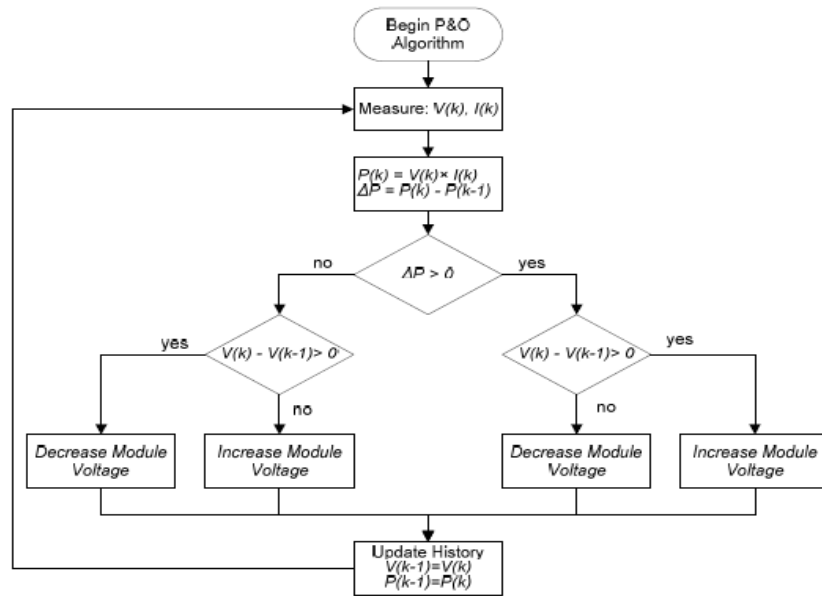


Figure 13. MPPT algorithm.

The simulation of the whole proposed system is done below.

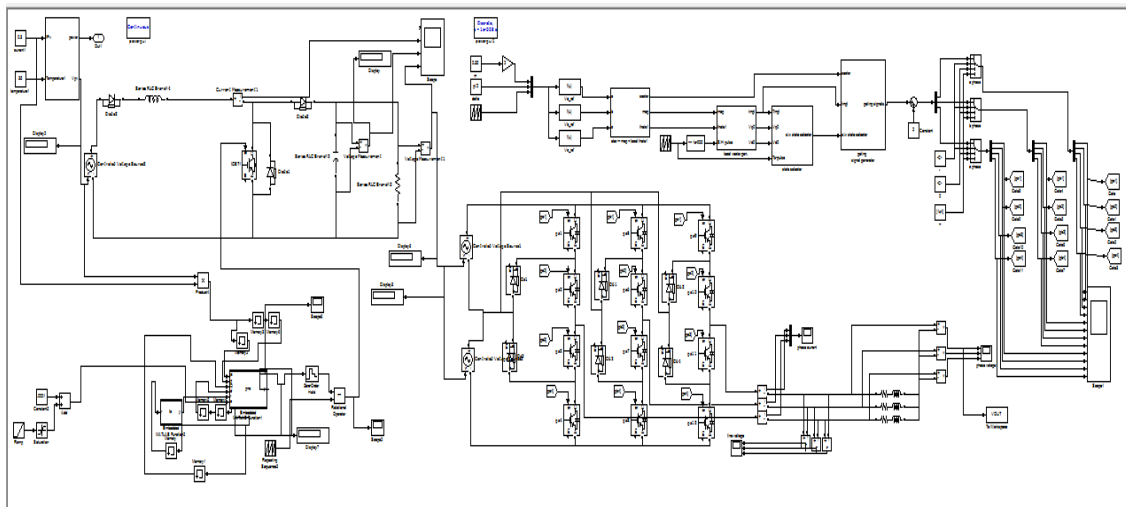


Figure 14. Simulation of the whole system implemented using MPPT algorithm.

6. Simulation Result

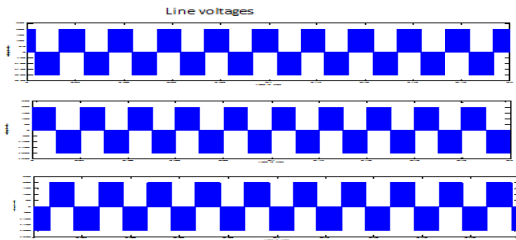


Figure. 15 phase voltages of two-level inverter

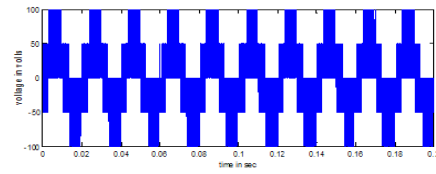
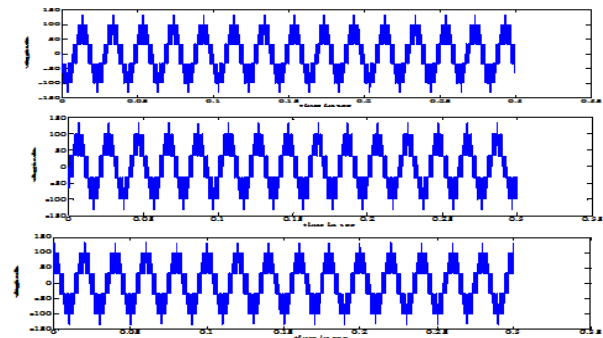
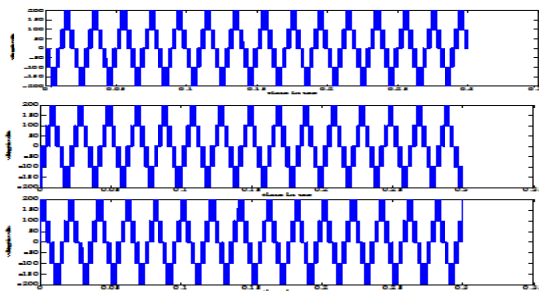


Figure. 16 line voltage of two-level inverter

Figure. 17 Line voltage of three-level SVPWM inverter Figure. 18 Phase voltage of three-level



SVPWM inverter

Line voltages and phase voltages of three-level SVPWM inverter are shown in figure 17 and figure 18.

7. Comparison of FFT analysis of two-level SVPWM and three-level SVPWM inverter

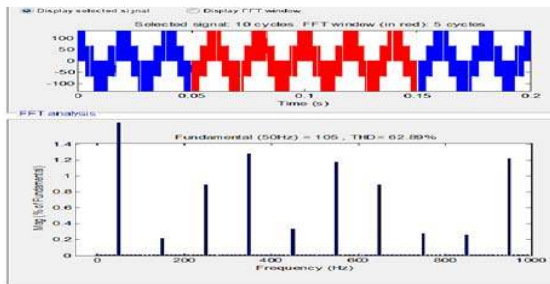


Figure 19. FFT analysis of two level inverter

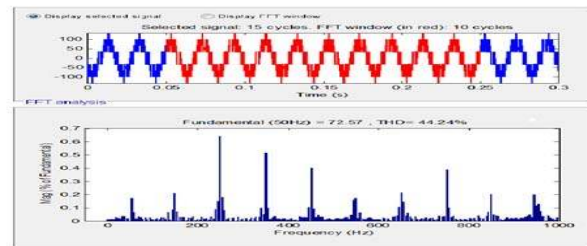


Figure 20. FFT analysis of three level inverter

Table 3. FFT Analysis of 2 & 3 level Inverter

| S.no | Level       | THD    |
|------|-------------|--------|
| 1.   | Two-level   | 62.89% |
| 2.   | Three-level | 44.24% |

The FFT analysis is done here in MATLAB Simulink. As we can see that the THD value decreases with as the no of levels increases. Further if we use a filter circuit then the THD value decreases to a very effective level.

### 8. Generation of pulses in SVPWM using Lab view

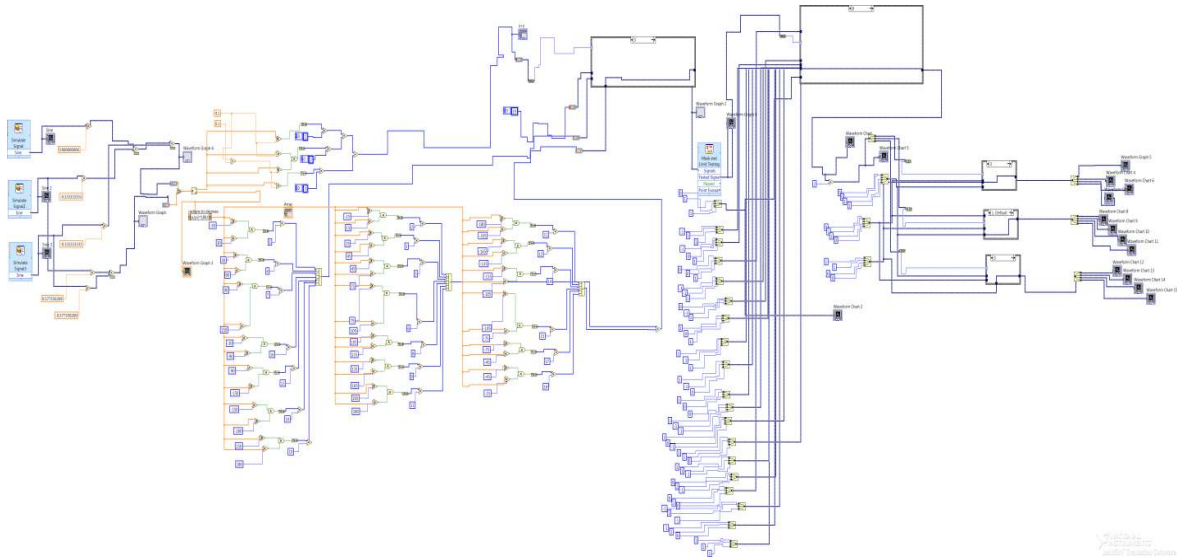


Figure 21. The generation of Pulses to fire the Mosfet

The generation of Pulses to fire the Mosfet is shown in Figure 21. This is done in accordance with the SVPWM technique.

### 9. Hardware Setup for 3-phase 3-level inverter

The whole hardware implementation is done here for the 3-level inverter. LabView is used here to generate the gate pulse and the optocoupler (TLP250) is used here to protect the gates from the negative spikes. The transformer set is also used here. While connected the whole circuit we got the output waveform of 3 phase 3 level inverter and by clicking on the MATH function on the DSO we got the FFT analysis in hardware.

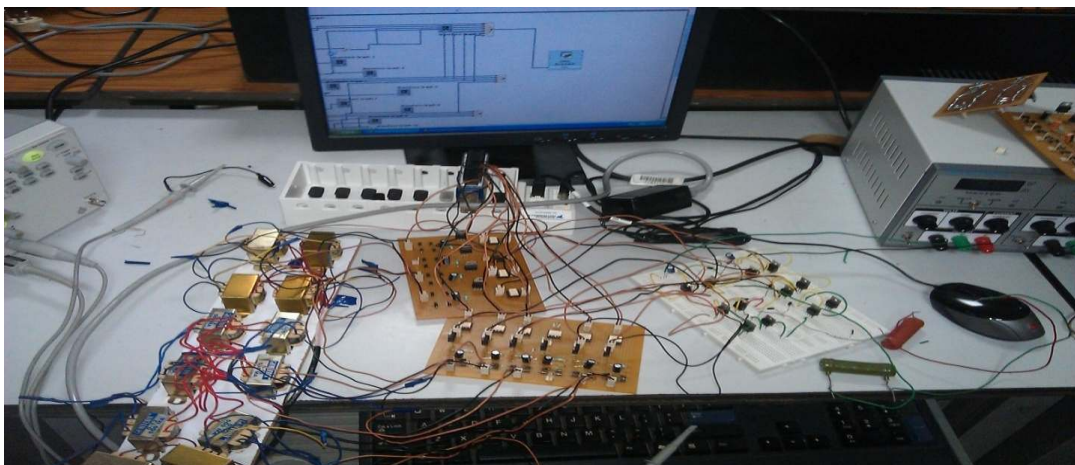
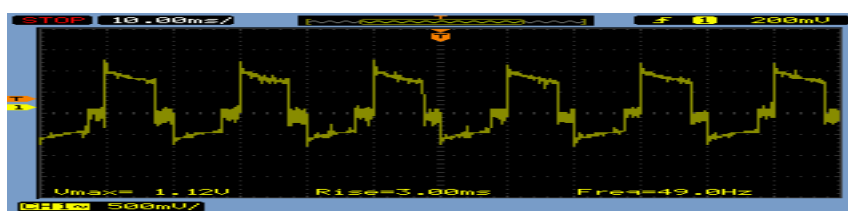
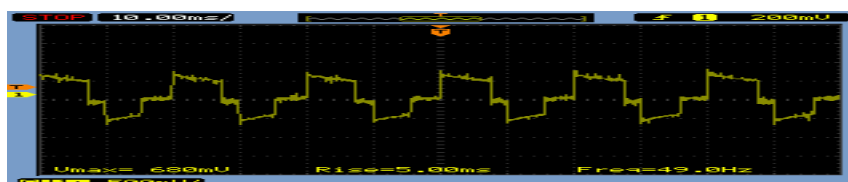


Figure 22. Hardware Setup for 3-phase 3-level inverter

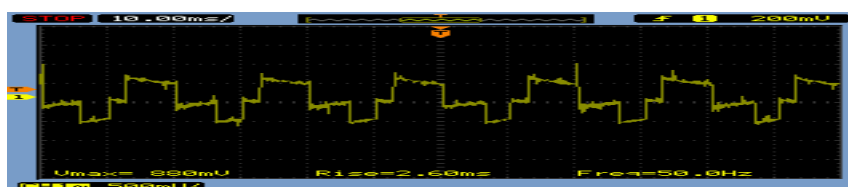
### Phase voltages of 3-level inverter



Phase A Voltage



Phase B Voltage



Phase C Voltage

Figure 22. Phase voltages of 3-level inverter

## 10. CONCLUSION

In this paper, the total Harmonics distortion of the two and three level inverter with SVPWM is analyzed by RL load. The simulations are done with MATLAB/SIMULINK. Hardware results are also verified with experimentation by using labview. The cost savings is further enhanced with the proposed diode-clamped inverters because of the significant reduction in the total VA ratings of the clamping diodes and in the total voltage rating of the voltage-splitting capacitors. These configurations may also be applied in distributed power generation involving photovoltaic cells, wind mills, fuel cells etc.

## ACKNOWLEDGEMENTS

I wish to thank our College VIT, University, Tamil Nadu for the wonderful facility and infrastructure provided to us to complete this project.

## REFERENCES

- [1] Z. Pan and F. Z. Peng, "Harmonics optimization of the voltage balancing control for multilevel converter/inverter systems", *IEEE Trans. Power Electron.*, vol. 21, no. 1, pp. 211–218, Jan. 2006
- [2] A. K. Gupta and A. M. Khambadkone, "A space vector PWM scheme for multilevel inverters based on two-level space vector PWM", *IEEE Trans. Ind. Electron.*, vol. 53, no. 5, pp. 1631–1639, Oct. 2006.
- [3] N. Dai, M. Wong, and Y. Han, "Application of a three-level NPC inverter as a three-phase four-wire power quality compensator by generalized 3DSVM", *IEEE Trans. Power Electron.*, vol. 21, no. 2, pp. 440–449, Mar. 2006.
- [4] Nguyen, T.H., P.K.W. Chan, Y. Shrivastava and S.Y.R. Hui, 2005. "A Three-Dimensional Space Vector Modulation Scheme for Three-Level Three-Wired Neutral Point Clamped Converters", *IEEE 36th Power Electronics Specialists Conference 2005*. pp. 2307-2314
- [5] Wenxi Yao, Haibung Hu, Zhengyu Lu, "Comparison of space vector modulation and carrier based modulation of multilevel inverter", *IEEE Trans., Power Electronics*, Vol.23, pp. 45 – 51, Jan 2008
- [6] Bosquets Monge. S, Bordonau. J., Rocabert. J, "A virtual vector pulse width modulation for a four level diode clamped DC-AC converter", *Power Electronics, IEEE Transaction*, Vol.23, pp.1964 -1972, July 2008
- [7] Sonal Sapra J.P Navani "Three level Inverter Using MAT LAB", *MIT International Journal of Electrical and Instrumentation Engineering* Vol. 1, No. 1, Jan 2011, pp 20-24